The International Journal of Biochemistry & Cell Biology 41 (2009) 1837–1845

Contents lists available at ScienceDirect

The International Journal of Biochemistry & Cell Biology

journal homepage: www.elsevier.com/locate/biocel

Review

Capacity of oxidative phosphorylation in human skeletal muscle New perspectives of mitochondrial physiology

Erich Gnaiger*

Department of General and Transplant Surgery, D. Swarovski Research Laboratory, Medical University of Innsbruck, Innrain 66/6, A-6020 Innsbruck, Austria

ARTICLE INFO

Article history:
Available online 2 April 2009

Keywords:
Mitochondrial respiratory control
High-resolution respirometry
Skeletal muscle
Q-cycle
Q-junction
Electron transport
Maximal oxygen consumption
Pyruvate
Glutamate
Succinate
Tricarboxylic acid cycle

ABSTRACT

Maximal ADP-stimulated mitochondrial respiration depends on convergent electron flow through Complexes I + II to the Q-junction of the electron transport system (ETS). In most studies of respiratory control in mitochondrial preparations, however, respiration is limited artificially by supplying substrates for electron input through either Complex I or II. High-resolution respirometry with minimal amounts of tissue biopsy (1–3 mg wet weight of permeabilized muscle fibres per assay) provides a routine approach for multiple substrate-uncoupler-inhibitor titrations. Under physiological conditions, maximal respiratory capacity is obtained with glutamate + malate + succinate, reconstituting the operation of the tricarboxylic acid cycle and preventing depletion of key metabolites from the mitochondrial matrix. In human skeletal muscle, conventional assays with pyruvate + malate or glutamate + malate yield submaximal oxygen fluxes at 0.50–0.75 of capacity of oxidative phosphorylation (OXPHOS). Best estimates of muscular OXPHOS capacity at 37 °C (pmol O_2 s^{-1} mg^{-1} wet weight) with isolated mitochondria or permeabilized fibres, suggest a range of 100–150 and up to 180 in healthy humans with normal body mass index and top endurance athletes, but reduction to 60–120 in overweight healthy adults with predominantly sedentary life style. The apparent ETS excess capacity (uncoupled respiration) over ADP-stimulated OXPHOS capacity is high in skeletal muscle of active and sedentary humans, but absent in mouse skeletal muscle. Such differences of mitochondrial quality in skeletal muscle are unexpected and cannot be explained at present. A comparative database of mitochondrial physiology may provide the key for understanding the functional implications of mitochondrial diversity from mouse to man, and evaluation of altered mitochondrial respiratory control patterns in health and disease.

Contents

Abbreviations: HRR, high-resolution respirometry; Imt, isolated mitochondria; Pfi, permeabilized fibers; P_{mt}, mitochondrial protein; SUIT, substrate-uncoupler-inhibitor-titration; TCA, tricarboxylic acid; u, uncoupled; W_w, wet weight (see also Table 1).

* Tel.: +43 512 504 24623; fax: +43 512 504 24625.
E-mail address: erich.gnaiger@i-med.ac.at.

1357-2725/$ – see front matter © 2009 Elsevier Ltd. All rights reserved.
doi:10.1016/j.biocel.2009.03.013

1. Introduction

Oxidative phosphorylation (OXPHOS) is a key element of bioenergetics, extensively studied to resolve the mechanisms of energy transduction in the mitochondrial electron transport system (ETS) and analyze various modes of mitochondrial respiratory control. Electrons flow to oxygen along linear thermodynamic cascades (electron transport chains (ETC)) from Complex I (CI) with three coupling sites, or from Complex II (CII) with two coupling sites (Chance and Williams, 1956). These pathways of electron transport are conventionally separated in studies of mitochondrial preparations, by using either NADH-linked substrates such as pyruvate + malate, or the classical succinate + rotenone combination, for analysis of site-specific H^+/e and ADP:O ratios (Chance and Williams, 1955; Lemasters, 1984; Mitchell and Moyle, 1967) and functional diagnosis of enzymatic defects in mitochondrial diseases. In mitochondrial physiology and pathology, maximal mitochondrial respiration in the coupled state is measured for quantitative determination of OXPHOS capacity, $J_{O_2,P}$ (see Table 1 for definition of symbols). Increasing evidence is available that mitochondrial density and thus $J_{O_2,P}$ per muscle mass is related to training and endurance exercise capacity (Andersen and Saltin, 1985; Blomstrand et al., 1997; di Prampero, 2003; Hoppeler et al., 1985; Starritt et al., 1999; Turner et al., 1997; Weibel and Hoppeler, 2005; Wibom et al., 1992; Zoll et al., 2002).

The methods and concepts established in bioenergetics are directly applied in numerous studies with a physiological perspective, considering that fluxes measured with 'succinate in the presence of ADP and phosphate should reflect the maximal physiological respiratory activity of mitochondria, since the rate-controlling steps of adenine nucleotide translocation and cytochrome *c* oxidation are involved' (Schwerzmann et al., 1989). Although it is generally appreciated that 'it is essential to define both the substrate and ADP levels in order to identify the steady-state condition of the mitochondria during the experiment' (Chance and Williams, 1956), surprisingly little attention is being payed in the majority of investigations to the question as to the most appropriate substrate for estimation of physiological oxidative capacity. Irrespective of the type of mitochondrial preparation, i.e. permeabilized fibres (Pfi) or isolated mitochondria (Imt), used to determine 'maximal ADP-stimulated respiration' (Saks et al., 1998; N'Guessan et al., 2004), some research groups prefer – appart from comparison with fatty acid oxidation – strictly pyruvate + malate as substrates (Tonkonogi et al., 1999; Mogensen et al., 2006), whereas others use only glutamate + malate 'to establish maximal oxidative capacities of mitochondria in muscles' (Daussin et al., 2008b). These and many other studies suggest (Table 2) that an important finding remained largely unnoticed, namely that ADP-stimulated respiration with pyruvate + malate and glutamate + malate yields only 66% and 75%, respectively, of $J_{O_2,P}$ observed with the substrate combination glutamate + succinate in pig skeletal muscle (Rasmussen et al., 1996). Identical results in human skeletal muscle (Rasmussen and Rasmussen, 2000) challenge the paradigm that pyruvate + malate or glutamte + malate are suitable and sufficient substrate combinations for evaluation of maximal physiological OXPHOS capacity, or that 'these measurements require the integrated function of the citric acid cycle' (Tonkonogi et al., 1999). On the contrary, the TCA cycle is functionally not 'closed' when using the substrate combination pyruvate + malate or glutamate + malate; depletion of citrate, isocitrate, 2-oxoglutarate and succinate into the incubation medium prevents any significant contribution of succinate oxidation to respiratory flux (Gnaiger, 2007). Reconstitution of TCA cycle function in mitochondrial preparations requires addition of succinate together with the conventional substrates for Complex I, to support the simultaneous, convergent electron flow through CI + II into the Q-junction (Fig. 1).

Table 1
Definition of terms and symbols.

Symbol	Additions[a]	Definition
ETS, State *E*	Substrates, uncoupler	Uncoupled state at optimal uncoupler concentration for maximum oxygen flux as a measure of electron transport system capacity (State 3u)
OXPHOS, State *P*	Substrates, ADP, P_i	ADP activated state at maximum oxygen flux as a measure of the capacity for oxidative phosphorylation (State 3)
LEAK, State *L*	Substrates, no ADP, oligomycin, atractyloside	Resting state of non-phosphorylating respiration when oxygen flux is maintained mainly to compensate for the proton leak after inhibition of ATP synthesis (States 4, 2′, 4o)
$J_{O_2,E}$, $J_{O_2,P}$ per tissue		Oxygen flux (pmol O_2 s^{-1} mg^{-1} wet weight) expressing tissue-ETS or tissue-OXPHOS capacity
$J_{O_2,E}$, $J_{O_2,P}$ per mt-marker		Oxygen flux (nmol O_2 s^{-1} mg^{-1} P_{mt}) expressing ETS or OXPHOS capacity per mitochondrial marker
$L/E = J_{O_2,L}/J_{O_2,E}$		*L*/*E* coupling control ratio; increases with uncoupling at constant ETS capacity
$P/E = J_{O_2,P}/J_{O_2,E}$		*P*/*E* coupling control ratio; decreases with limitation by the phosphorylation system
$L/P = (L/E)/(P/E)$		*L*/*P* coupling control ratio; 1/RCR
CI electron input	PM, GM, PMG	Electron input into the Q-junction through Complex I (NADH-related substrates)
CII electron input	S(Rot)	Electron input into the Q-junction through Complex II (succinate)
CI + II electron input	PMS, GMS, GS	Electron input into the Q-junction through Complex I + II (CI + II substrate combination)
$FCR = J_i/J_{ref}$		Flux control ratios; fluxes in various states *i* normalized to a common reference state, J_{ref}
$CCR = J_i/J_{ref}$	Constant substrate	Coupling control ratios, FCR with J_i and J_{ref} in the same substrate state
$SCR = J_i/J_{ref}$	Constant coupling	Substrate control ratios, FCR with J_i and J_{ref} in the same coupling state
ROX	Rotenone + myxothiazol	Residual oxygen consumption, subtracted from total flux

[a] G, glutamate; M, malate; P, pyruvate; S or S(Rot), succinate + rotenone.

Extending the concept on mitochondrial respiratory control by multiple substrate supply (Rasmussen et al., 1996, 2001a,b; Rasmussen and Rasmussen, 2000), a novel perspective of mitochondrial respiratory physiology emerges from a series of studies based on high-resolution respirometry (HRR; Gnaiger et al., 1995; Gnaiger, 2001, 2008). Application of permeabilized muscle fibres (Veksler et al., 1987; Letellier et al., 1992) has become successful to minimize the size of needle biopsies and reduce the amount of tissue required for HRR. Long-term stability of the instrumental

Table 2
Tissue-OXPHOS capacity in Vastus lateralis of healthy humans. Normal, overweight and obese groups are defined according to average body mass index (BMI)[a]. Subjects are ranked by declining fitness level and increasing average age. Within BMI groups, studies are distinguished with high (A) and low OXPHOS capacity (B; comp. Fig. 3). M/F, number of males and females in each study. Irrespective of measurements with isolated mitochondria (Imt) or permeabilized muscle fibres (Pfi), OXPHOS capacity, $J_{O_2,P}$ (ADP-activated oxygen flux), is expressed per wet weight, W_w, of muscle tissue (pmol O_2 s^{-1} mg^{-1}) and adjusted to 37 °C.[b] $J_{O_2,P}$ is also given per mitochondrial protein, P_{mt} (nmol O_2 s^{-1} mg^{-1}). Substrate control of $J_{O_2,P}$, with electron entry through Complex I (CI; PM, pyruvate + malate or GM, glutamate + malate) or Complex II (CII; S, succinate + rotenone), and with convergent electron input through Complexes I + II (CI + II).

Fitness level[a]	Age (years)	M/F	T_{exp} (°C)	Preparations	$J_{O_2,P}$ CI (PM)	$J_{O_2,P}$ CI (GM)	$J_{O_2,P}$ CII (S)	$J_{O_2,P}$ CI + II (per W_w)	$J_{O_2,P}$ CI + II (per P_{mt})	P_{mt}/W_w (μg/mg)	References[c]
Normal (BMI 20–25)											
A											
Athletic	31	15/0	22	Pfi	–	132	–	(181)[d1]		(15.4)[e1]	1[f]
Athletic	36	7/0	22	Pfi	117	116	148	(173)[d2]		(14.8)[e1]	2[f]
Athletic	41	11/2	22	Pfi	–	106	–	(146)[d1]		(12.4)[e1]	3[f]
Trained	25	9/0	25	Imt	92	–	–	(144)[d3]		(12.2)[e1]	4
Active	47	8/2	22	Pfi	–	101	–	(138)[d1]		(11.7)[e1]	5[f]
Ath. to Sed.	24	18/0	25	Imt	79	90	103	123	11.8	10.5	6
Ath. to Sed.	24	12/0	25	Imt	75	90	100	(121)[d2]	11.7	10.3	7[g]
Untrained	27	5/3	25	Imt	63	–	–	(98)[d3]		(8.3)[e1]	8
	32 ± 9[h]	85/7						140 ± 27		11.9 ± 2.3	
B											
Active	24	10/0	25	Imt	49	–	–	(77)[d3]		(6.6)[e1]	9
			25	Pfi	57	–	–	(90)[d3]		(7.6)[e1]	9
Active	27	10/0	25	Pfi	53	–	–	(83)[d3]		(7.0)[e1]	10
Ath. to Sed.	29	10/0	25	Imt	48	–	–	(75)[d3]		(6.4)[e1]	11
Untrained	26	4/4	25	Pfi	45	–	–	(70)[d3]		(6.0)[e1]	12
Sedentary	23	7/7	37	Pfi	–	26	57_E	54		(4.6)[e1]	13
Sedentary	25	5/0	30	Pfi	–	57	–	(79)[d1]		(6.7)[e1]	14[f]
	26 ± 2[h]	46/11						75 ± 11		6.4 ± 1.0	
Overweight (BMI 25–30)											
A											
Active	46	6/2	22	Pfi	–	79	–	(109)[d1]		(10.5)[e2]	3[f]
Act. to Sed.	72	10/1	25	Imt	68	83	104	(115)[d2]	10.4	11.1	7
Untrained	24	9/0	25	Imt	65	–	–	(102)[d3]		(9.8)[e2]	4
Sedentary	41	7/0	22	Pfi	74	44	81	(91)[d2]		(8.8)[e2]	2[f]
Sedentary	45	7/4	22	Pfi	–	44	–	(61)[d1]		(5.9)[e2]	15[f]
Sedentary	47	8/0	22	Pfi	–	50	–	(68)[d1]		(6.6)[e2]	3[f]
Sedentary	51	10/1	22	Pfi	–	43	–	(58)[d1]		(5.6)[e2]	5[f]
Sedentary	52	8/1	22	Pfi	–	46	–	(63)[d1]		(6.1)[e2]	16[f]
Sedentary	55	6/1	22	Pfi	–	34	56	(57)[d4]		(5.5)[e2]	17[f]
Sedentary	58	8/0	37	Pfi	–	43	76_E	85		(8.2)[e2]	18
	49 ± 12[h]	79/10						81 ± 22		7.8 ± 2.1	
B											
Sedentary	59	16/0	37	Pfi	–	–	–	27		(2.6)[d2]	19
Sedentary	75	7/7	37	Pfi	–	22	45_E	44		(4.2)[d2]	13
Obese (BMI >30)											
Sedentary	54	11	37	Pfi	–	29	–	61		(5.2)[e2]	20

[a] BMI = body weight/height^2 (kg/m^2); fitness levels according to subject description or ergometric respiratory capacity ($\dot{V}_{O_2,max}$), Ath. to Sed. indicates the average of a large range from athletic to sedentary.

[b] Data obtained at experimental temperature, T_{exp}, were multiplied by a T-factor corresponding to a Q_{10} of 2 (multiplication factor for a 10 °C difference). For T_{exp} of 22 °C, 25 °C and 30 °C, the T-factor is 2.83, 2.30 and 1.62, respectively.

[c] References and notes: (1) Ponsot et al. (2005). (2) Daussin et al. (2008b). (3) Zoll et al. (2002). (4) Mogensen et al. (2006), 15–16% mt-yield. (5) Mettauer et al. (2001). (6) Rasmussen and Rasmussen (2000) and Rasmussen et al. (2001a,b, 2004), $J_{O_2,P}$(CI + II) measured with GS; 45% mt-yield. (7) Rasmussen et al. (2003), 47% and 37% mt-yield in 20+ and 70+ age group. (8) Bakkman et al. (2007); 23% mt-yield. (9) Tonkonogi et al. (1999), 28% mt-yield. (10) Tonkonogi et al. (1998). (11) Tonkonogi and Sahlin (1997), 26% mt-yield. (12) Walsh et al. (2001). (13) Hütter et al. (2007), CI and CI + II measured in the presence of 1 mM octanoylcarnitine with GM and GMS, a significant cytochrome *c* effect on respiration is observed in this study, but not in Boushel et al. (2007) and Rabøl et al. (2009). (14) Anderson et al. (2009), the respiration medium includes benzyltoluene sulfonamide as an inhibitor of contraction, age is the middle of the range (18–31 years). (15) Daussin et al. (2008a). (16) Garnier et al. (2005). (17) Echaniz-Laguna et al. (2002), CI + II is calculated as the average of GM/0.73 and S/0.83. (18) Boushel et al. (2007), CI + II measured with GMS. (19) Phielix et al. (2008), CI + II measured with GMS. (20) Rabøl et al. (2009), CI in state PMG, CI + II in state PMGS.

[d] Flux not measured in the CI + II substrate state, but calculated on the basis of CI/CI + II and CII/CI + II substrate control ratios at 25 °C (Fig. 2). [d1] $J_{O_2,P}(CI+II) = J_{O_2,P}(GM)/0.73$; [d2] $J_{O_2,P}(CI+II)$ is the average of $J_{O_2,P}(PM)/0.64$, $J_{O_2,P}(GM)/0.73$ and $J_{O_2,P}(S+Rot)/0.83$; [d3] $J_{O_2,P}(CI+II) = J_{O_2,P}(PM)/0.64$; [d4] $J_{O_2,P}(CI+II)$ is the average of GM/0.73 and S/0.83.

[e] Mitochondrial protein content (μg P_{mt}/mg W_w) calculated from $J_{O_2,P}$(CI + II) per W_w, assuming a constant mt-OXPHOS capacity, [e1] for normal BMI: 11.8 nmol s^{-1} mg^{-1} P_{mt} (from ref. 6); [e2] for overweight and obese: 10.4 nmol s^{-1} mg^{-1} P_{mt} (from Rasmussen et al. (2003)).

[f] Fibre wet weight to dry weight ratio is assumed to be 3.5 (N'Guessan et al., 2004).

[g] Mitochondrial protein content is 10.3 mg g^{-1}.

[h] Average ± SD for the group of studies, and total number of males and females involved.

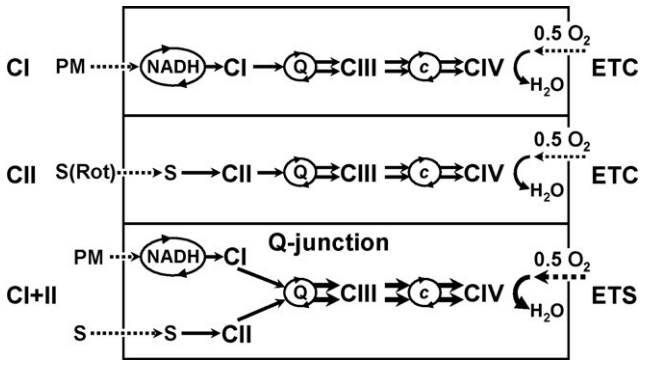

Fig. 1. Substrate control of electron flow to oxygen through Complex I or II separately (CI or CII), or simultaneously (CI + II) in mitochondrial preparations. Substrate supply restricted to pyruvate + malate, PM, or succinate + rotenone, S(Rot) exerts artificial upstream control of flux through the linear electron transport chain. With PM (or GM) as substrates, metabolite depletion (loss of citrate, isocitrate, 2-oxoglutarate and succinate from the matrix) prevents substrate supply to CII. With succinate as the only substrate, blockage of CI is necessary to prevent inhibition of succinate dehydrogenase by accumulating oxaloacetate. Combined CI + II substrate supply with simultaneous electron entry at the Q-junction exerts an additive effect on total electron flux through the convergent electron transport system. This shifts control of flux downstream towards Complexes III and IV, and towards the phosphorylation system in oxidative phosphorylation. Convergent electron flow corresponds to the operation of the tricarboxylic acid cycle in the intact cell, generating simultaneously NADH and succinate in the matrix as substrates for CI + II. This physiological state is reconstituted in mitochondrial preparations by external CI + II substrate supply (PMS; or substituting pyruvate by glutamate, GMS or GS). Substrate entry across the inner mitochondrial membrane into the mitochondrial matrix space is shown by dotted arrows (metabolite depletion from the matrix is not shown). Full arrows indicate flow of electron pairs (single arrows) split into flow of single electrons (double arrows).

signal and of mitochondrial preparations in mitochondrial respiration medium MiR05 (Gnaiger et al., 2000a), and high dilution of the sample in the oxygraph chamber provide the experimental basis for application of sequential, multiple substrate-uncoupler-inhibitor titration (SUIT) protocols (Gnaiger et al., 2005). The design of SUIT protocols places a balanced emphasis on coupling control and substrate control of OXPHOS capacity, for exploring the functional consequences of convergent mitochondrial pathways at the Q-junction (Gnaiger, 2007). Following this integrated systems approach, combining HRR with application of permeabilized fibres, incubation in optimized medium MiR05, measurement at physiological temperature and strategic design of CI + II SUIT protocols, a rapidly growing number of studies confirms the importance of the additive effect of substrate combinations on $J_{O_2,P}$ (Aragonés et al., 2008; Boushel et al., 2007; Hütter et al., 2007; Jüllig et al., 2008; Lemieux et al., 2006; Phielix et al., 2008; Rabøl et al., 2009; Wijers et al., 2008).

2. Respirometry with permeabilized fibres and isolated mitochondria

2.1. High-resolution respirometry compared to specialized microchamber system

Respiration of permeabilized muscle fibres was measured by high-resolution respirometry with the Oxygraph-2k (OROBOROS INSTRUMENTS, Innsbruck, Austria) at 37 °C, using 1–3 mg tissue wet weight in each 2 ml glass chamber (Boushel et al., 2007). Respiration of isolated mitochondria was measured in a 36.5 μl glass microchamber at 25 °C, with 3–15 μg mitochondrial protein (P_{mt}) (Rasmussen and Rasmussen, 2000). At a yield in mitochondrial isolation of 45%, and a mitochondrial protein concentration of 10 μg P_{mt}/mg tissue wet weight, this corresponds almost exactly to the same amount of biopsy tissue (0.7–3.3 mg wet weight) required per experimental run in the two approaches. In HRR, however, the tissue concentrations (or concentrations of P_{mt}) in the chamber are low, at 0.5–1.5 mg wet weight/ml (approximately 0.005–0.015 mg P_{mt}/ml; or 5–15 μg/ml), compared to high sample concentrations in the microchamber, equivalent to 8–40 mg wet/ml (0.08–0.4 mg P_{mt}/ml). High sample concentrations in the chamber yields high volume-specific oxygen fluxes, which are necessary if noise of the oxygen sensor limits the resolution of low fluxes. Then the oxygen concentration in the respirometer chamber is exhausted within a few minutes, restricting the experiment to simple protocols with few titration steps. Sample dilution is possible in HRR, requires a well-adjusted medium to prevent mitochondrial deterioration, and is required for application of extended SUIT protocols (Gnaiger et al., 2005; Gnaiger, 2008).

2.2. Respiration per muscle mass

Muscle- or tissue-OXPHOS capacity is mitochondrial respiratory capacity, $J_{O_2,P}$, per muscle mass. Fibre wet weight can be easily determined (Mettler Toledo microbalance XS205DU) immediately before addition of the sample into the oxygraph chamber, which permits online recording of oxygen flux per unit tissue mass (OROBOROS DatLab software). Measurement of dry weight, in contrast, depends on the complete recovery of the tissue from the experimental chamber. This and variable specific water content contribute to the scatter of respiration per muscle mass, and may explain the large range of wet to dry weight ratios reported for human Vastus lateralis, from 3.3 (Tonkonogi and Sahlin, 1997), 3.5 (N'Guessan et al., 2004), and 6.2, 6.5 to 6.9 (Kunz et al., 1993; Kunz et al., 2000; Saks et al., 1998). Each incubation of permeabilized fibres is an independent measurement with a separate tissue sample (ca. 2 mg) obtained from a small biopsy. Replicate measurements with Pfi, therefore, include the intraindividual variability of tissue heterogeneity (Kuznetsov et al., 2002). Mitochondrial concentration (amount per tissue mass) is the major determinant of tissue heterogeneity on the mg-scale, but heterogeneity of mitochondrial injuries can be detected within muscle fibres (Kuznetsov et al., 2004). In addition to respirometric errors, accuracy depends on fibre preparation, such as elimination of non-muscular components (connective tissue, microcapillaries), permeabilization (Saks et al., 1998) and measurement of muscle mass.

These methodological considerations point to a fundamental difference of replicate respirometric measurements and different titration protocols performed in parallel incubations with Pfi and Imt, which is important for statistical evaluation of reproducibility. Respiration of isolated mitochondria is measured on subsamples from the homogenate of Imt prepared from a large biopsy of a patient (the minimum is ca. 100 mg; Rasmussen and Rasmussen, 2000). Replicate measurements with Imt, therefore, reflect exclusively the methodological accuracy of respirometric measurements, unrelated to mitochondrial yield, density and heterogeneity in the tissue. Flux control ratios obtained from sequential titrations within a single protocol with Pfi, therefore, are comparable with flux ratios obtained from parallel titration protocols with Imt. When using isolated mitochondria, the mitochondrial yield must be quantified to convert mitochondrial OXPHOS capacity (mt-OXPHOS, $J_{O_2,P}$ per unit mt-marker) to tissue-OXPOHOS capacitiy (Table 2).

2.3. Experimental conditions for maximal flux

Concentrations of TCA cycle intermediates do not limit respiration in contracting skeletal muscle (Dawson et al., 2005), and the initial increase during exercise is not essential for activation of respiration (Bangsbo et al., 2006). Similarly, substrates are supplied at saturating concentrations (Ponsot et al., 2005) for measurement of respiratory capacity of mitochondrial preparations. 0.2 mM ADP

does not fully saturate flux in isolated mitochondria (Puchowicz et al., 2004; Gnaiger, 2001), and high [ADP] concentrations are required particularly in permeabilized fibres to overcome limitations by diffusion and by the tubulin-regulated conductance of the outer mitochondrial membrane (Rostovtseva et al., 2008). In permeabilized muscle fibre bundles of high respiratory capacity, the apparent K_m for ADP increases up to 0.5 mM (Saks et al., 1998). This implies that >90% saturation is reached only at >5 mM ADP, yet few studies use such high ADP concentrations in permeabilized muscle fibres, and lack of stimulation at 2.5 mM ADP by increasing [ADP] provides evidence for lower $K'_{m,ADP}$. Maximal aerobic capacity *in vivo* is limited by oxygen supply (di Prampero, 2003; Mitchell and Saltin, 2003; Richardson et al., 1999), but respiratory capacity of mitochondrial preparations must be evaluated at kinetic oxygen saturation, comparable to the application of saturating ADP concentrations for measuring $J_{O_2,P}$. Even at 20 μM, oxygen does not limit respiration of isolated mitochondria and small cells (20–50-fold above the c_{50} or K'_{m,O_2}; Gnaiger et al., 1998, 2000b; Scandurra and Gnaiger, 2009). In permeabilized muscle fibre bundles, however, diffusion restriction increases the sensitivity to oxygen supply 100-fold (rat soleus and rat heart; Gnaiger, 2003). Oxygen limitation of respiration in permeabilized fibres is prevented by maintaining oxygen levels in the respirometer above air saturation in the range of 500–200 μM (Boushel et al., 2007; Aragonés et al., 2008). Lack of attention to experimental oxygen limitation of Pfi, however, partly explains apparent low specific activities (Table 2).

3. Convergent CI + II electron input and OXPHOS capacity

3.1. Reconstitution of TCA cycle function

In addition to coupling and substrate supply, metabolite depletion of TCA cycle intermediates plays a fundamental role in OXPHOS flux control in isolated mitochondria or permeabilized cells. Using classical NADH-related substrates such as pyruvate, malate and glutamate, the TCA cycle metabolites citrate and 2-oxoglutarate are exchanged rapidly for malate by the tricarboxylate and 2-oxoglutarate carrier, and succinate is lost from the matrix space in exchange for inorganic phosphate catalyzed by the dicarboxylate carrier (Gnaiger, 2007). Evaluation of the functional design of the OXPHOS system requires a conceptual transition from analyses of the electron transport chain to a perspective of the convergent structure of electron flow to the Q-junction in the mitochondrial electron transport system (Fig. 1). The convergent structure of the ETS is functionally related to substrate compartmentation and mitochondrial network organization (Benard et al., 2007, 2008). Molar ratios of redox components of the ETS cannot be understood in terms of a linear chain (Fig. 1; ETC CI and CII). Instead, the sum of redox components upstream of the Q-cycle (the convergent input branches) is related to the linear sequence of redox components downstream of the Q-junction (Fig. 2; ETS CI + II). Consequently, the excess capacity of Complexes III and IV is high when related to CI or CII electron input (Benard et al., 2008; Gnaiger et al., 1998; Rossignol et al., 2003). These apparent excess capacities are in part explained functionally, as a necessary requirement for higher capacities of the Q-cycle and respiratory complexes downstream of Q, which have to match the sum of the partial capacities of all contributory branches converging at the Q-junction (Fig. 2; CI + II).

A 'substrate cocktail' (NADH + glutamate + malate + succinate) activates in mitochondria of fungi not only convergent CI + II electron input, but in addition the alternative NADH-ubiquinone oxidoreductase which together support a high oxygen flux, whereas flux with NADH, pyruvate or malate alone is 0.85, 0.14 and 0.17 of flux with the substrate cocktail (Tudella et al., 2003). No conclusions can be drawn on the additive effect of convergent pathway

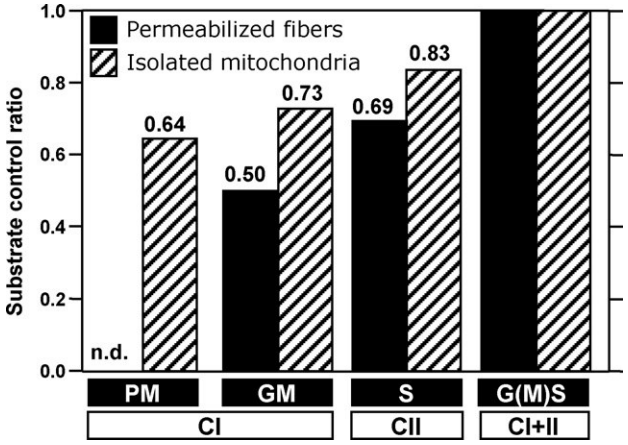

Fig. 2. Substrate control ratios in permeabilized fibers and isolated mitochondria incubated with substrates for electron supply through Complex I (CI; pyruvate + malate or glutamate + malate), CII (succinate + rotenone), and with convergent CI + II electron supply (glutamate + malate + succinate or glutamate + succinate) as the references state. Fluxes relate to OXPHOS capacity (State 3) with saturating [ADP], except for the CII/CI + II ratios in Pfi, where CII_E provides the estimate of CII_P (Table 2; data from Boushel et al., 2007; and Rasmussen et al., 2001a,b). n.d., Not determined.

fluxes, since pyruvate or malate alone are insufficient for activation of flux through Complex I; the reaction stops at the point of citrate synthase which requires simultaneously acetyl CoA formed from pyruvate and oxaloacetate formed from malate. It is essential that reconstitution of partial TCA cycle activity is considered at the level of each contributory pathway. Whereas NADH supports a proper pathway in mitochondria with an alternative NADH-ubiquinone oxidoreductase facing the outer side of the inner membrane, malate alone does not. This concept (pyruvate + malate) is fully established in bioenergetics on the level of electron entry through a single pathway (Fig. 2, ETC), and is simply extended to the level of multiple pathways converging at the Q-junction (Fig. 2, ETS).

Convergent electron transport corresponds to the operation of the TCA cycle and mitochondrial substrate supply *in vivo*. In mitochondrial preparations, conventional measurements of active respiration (State 3; $J_{O_2,P}$ with saturating concentrations of inorganic phosphate and ADP) underestimate OXPHOS capacity when restricting substrate supply to pyruvate + malate, glutamate + malate or succinate + rotenone. Substrate control ratios (SCR) are flux ratios normalized with respect to a common reference state of substrate supply, expressing the relative control exerted by variation of experimental substrates at a fixed coupling state (Fig. 2).

The SUIT protocol applied for permeabilized fibres (Boushel et al., 2007) can be summarized as,

$$e_N + M + G_{+D} + c + S_{+u} + (Rot) \quad (1)$$

'+' Signs separate respiratory states observed after titrations. The substrates are endogenous (e), malate (M; 2 mM), glutamate (G; 10 mM), cytochrome *c* (*c*; 10 μM) and succinate (S; 10 mM). The inhibitor rotenone (Rot; 0.5 μM) is shown in parentheses. Titrations related to coupling control are indicated by subscripts: no added adenylates (N), ADP (D; 2.5 mM) and uncoupler FCCP (u; optimum concentration for maximal flux). The first OXPHOS state is observed with GM (CI; Fig. 2). The subsequent cytochrome *c* test yields information on the intactness of the outer mitochondrial membrane, since no stimulation of respiration was observed (see Kuznetsov et al., 2004). The next state is obtained after a substrate control step from CI_P to $CI + II_P$ (in the OXPHOS state; reference state in Fig. 2). Coupling control from OXPHOS to ETS capacity, $J_{O_2,P}$ to $J_{O_2,E}$, is evaluated by uncoupler titration ($CI + II_E$). Inhibition of CI by rotenone shows substrate control from $CI + II_E$ to CII_E. Only OXPHOS states are considered in Fig. 2, for evaluation of SCR in the coupled state,

except for CII_P which has not been measured (protocol 1) but is estimated on the basis of CII_E (see Table 1 for definition of terms).

3.2. Oxidative phosphorylation versus electron transport system: coupling and substrate control ratios

Importantly, the SCR for OXPHOS capacity (Fig. 2; State *P*) differ from the SCR for the same substrate in the uncoupled State *E* (ETS capacity), since the phosphorylation system exerts control over coupled respiration and limits $J_{O_2,P}$ relative to $J_{O_2,E}$. This is the case in human skeletal muscle (the $J_{O_2,P}/J_{O_2,E}$ or P/E coupling control ratio is 0.7–0.8 with CI + II; Boushel et al., 2007; Rasmussen et al., 2001a), rat skeletal muscle respiring with pyruvate + malate (P/E = 0.56; Benard et al., 2008; 0.88; Johnson et al., 2006; Scheibye-Knudsen and Quistorff, 2009), but not in mouse skeletal muscle mitochondria (P/E = 1 with CI + II substrates; Aragonés et al., 2008). Although the phosphorylation system (adenine nucleotide translocase, phosphate transporter, ATP synthase) limits $J_{O_2,P}$(CI) and particularly $J_{O_2,P}$(CI + II) in human muscle mitochondria, this is not necessarily the case with succinate + rotenone. The phosphorylation flux is much lower with succinate, due to the lower ADP:O ratio with CII compared to CI and lower $J_{O_2,P}$(CII) compared to $J_{O_2,P}$(CI + II). Then the capacity of the phosphorylation system is sufficient to maintain the P/E ratio close to (0.93; Rasmussen et al., 2001b; 25 °C) or not significantly different from 1.0 (Gnaiger et al., 2005; 30 °C) with succinate + rotenone in human skeletal muscle mitochondria.

Substrate control ratios shown in Fig. 2 express the additive effect of combined CI + II substrate supply. The general flux control pattern is identical in Pfi and Imt (Fig. 2). At present it is impossible to identify the causes that may be responsible for the lower SCR for GM/GMS and S/GMS in Pfi (0.50 and 0.69) compared to the SCR for GM/GS and S/GS in Imt (0.73 and 0.83; Fig. 2). These variations may result from different experimental conditions (respiration media; 37 °C versus 25 °C) and sample preparation, or the SCR reflect actual differences of mitochondrial quality in the two study groups (fitness levels, age; Table 2).

3.3. Permeabilized fibres and isolated mitochondria

In human Vastus lateralis, rat skeletal muscle and rat heart, $J_{O_2,P}$ of permeabilized fibres is 0.86, 0.92 and 0.87 of flux in isolated mitochondria (Kunz et al., 1993; Veksler et al., 1987). In other studies, a 1.16- and 1.22-fold higher respiration is obtained in Pfi compared to Imt in human Vastus lateralis (Tonkonogi et al., 1999) and rat skeletal muscle (Scheibye-Knudsen and Quistorff, 2009). Taken together, both types of mitochondrial preparation (Pfi and Imt) yield within experimental error comparable estimates of OXPHOS capacity when normalized to tissue mass or P_{mt}. This conclusion is further supported by the data summarized in Table 2. The quantitative agreement of mitochondrial respiratory capacity derived from Pfi and Imt establishes a close link between studies of Pfi and Imt, in contrast to the separation of proponents of Pfi versus Imt. (i) Despite low mitochondrial yields in the range of 15–45% (Table 2), the fraction of mitochondria obtained in Imt is representative of the entire mitochondrial population retained in Pfi. (ii) The additive effect of convergent CI + II electron flow applies equally to Pfi and Imt. In general, therefore, the apparent excess capacity of cytochrome *c* oxidase (CIV) is lower with reference to the higher flux in the CI + II substrate state (GMS) compared to a CI substrate state (GM; Table 2). This has been interpreted as a salient feature of respiratory capacity in permeabilized fibres versus isolated mitochondria (Kunz et al., 2000; in contrast to Kunz et al., 1993). The apparent CIV excess capacity (comparable to SCR in general) depends on the reference state (Gnaiger et al., 1998; Rossignol et al., 2003). When CI or CII substrate supply is taken as the reference state with an artificially limited OXPHOS capacity, then the apparent CIV excess capacity is increased, whereas it declines relative to the high CI + II OXPHOS capacity, which is independent of Pfi or Imt as shown by the statistical identity of absolute fluxes (Table 2) and similarity of substrate control ratios (Fig. 2).

4. Tissue-OXPHOS capacity in human permeabilized muscle fibres and isolated mitochondria

Few studies on human muscle mitochondria apply physiological conditions for estimating mitochondrial OXPHOS capacity. In Table 2, a physiological reference state is defined with CI + II substrate supply (Fig. 2) at experimental temperature close to body temperature, for quantitative evaluation of $J_{O_2,P}$ in mammalian tissues. The further the experimental conditions differ from the physiological reference state, the larger the error becomes which may result from adjustment to the CI + II substrate state and 37 °C, applying the substrate control ratios from Fig. 2 and a commonly assumed temperature coefficient (Table 2). Among 20 publications, five report $J_{O_2,P}$ with convergent electron transport based on CI + II substrate supply, and the most frequently chosen experimental temperatures are 25 °C or even 22 °C (Table 2). To summarize results obtained under such a wide and inhomogenous range of experimental conditions, only healthy control groups are considered where anthropometric information is available to assess fitness levels (Table 2).

Any diagnostic evaluation of OXPHOS capacity in patients requires comparison with healthy controls who are carfully matched 'not only for age, but also for physical activity using cyclo-ergometric incremental exercise tests with measure of oxygen uptake to determine fitness level of patients and controls' (Echaniz-Laguna et al., 2002). To the same extent, comparison of different studies on healthy subjects requires a matching of fitness levels. If the technically more involved ergometric tests are not available, the body mass index provides a generally accessible anthropometric index of fitness. Accordingly, subjects were grouped into normal, overweight and obese (Table 2). Highest $J_{O_2,P}$ of 150–180 pmol O_2 s^{-1} mg^{-1} wet weight were calculated for athletes. Within the group of normal average body mass index, the average tissue-OXPHOS capacity for a wide range of athletic to sedentary fitness levels (123 pmol O_2 s^{-1} mg^{-1}; Rasmussen et al., 2001a,b, 2004; Rasmussen and Rasmussen, 2000) is in good agreement with 138 and 144 pmol O_2 s^{-1} mg^{-1} in the active or trained groups studied by Mettauer et al. (2001) and Mogensen et al. (2006), comparing results with Imt and Pfi adjusted from different temperatures and protocols (Table 2). The active and trained groups have higher tissue-OXPHOS capacity than the untrained (Table 2, Normal – A).

Variations of fitness level explain to a large extent the range of tissue-OXPHOS capacities in healthy controls (Table 2). A direct relationship between aerobic exercise capacity and $J_{O_2,P}$ has been reported by several authors (Rasmussen et al., 2001b; Tonkonogi and Sahlin, 1997; Mettauer et al., 2001; Zoll et al., 2002; Daussin et al., 2008b). Comparison of tissue-OXPHOS capacity adjusted to a common physiological reference state and maximal whole body oxygen uptake reveal quantitative agreement between several study groups, but also show discrepancies which may identify some cases of low mitochondrial respiratory capacity as possible outliers (Fig. 3). Numerous potential artefacts are known to reduce mitochondrial respiration (Rasmussen and Rasmussen, 1997), whereas systematic errors rarely cause an overestimation of oxygen flux. High tissue-OXPHOS capacities and an identical dependence on maximal whole-body oxygen uptake are obtained with permeabilized fibres (Mettauer et al., 2001; Zoll et al., 2002) and isolated mitochondria (Mogensen et al., 2006) (Fig. 3). The low

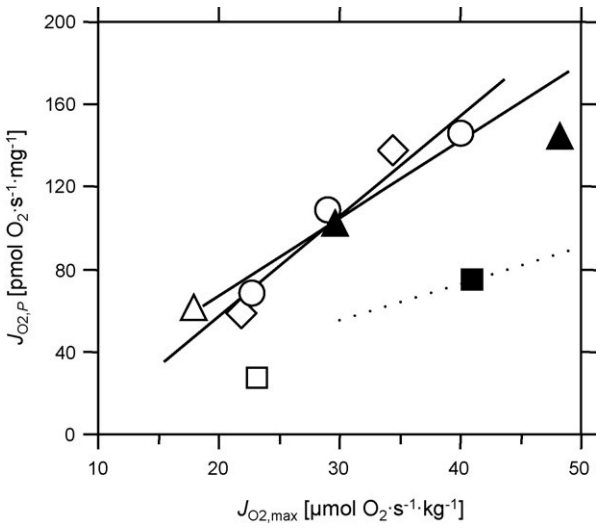

Fig. 3. OXPHOS capacity, $J_{O_2,P}$ (pmol s^{-1} mg^{-1} = µmol s^{-1} kg^{-1}) in human Vastus lateralis (per mg wet weight; adjusted to 37 °C and CI + II substrate supply) as a function of whole body respiratory capacity, $J_{O_2,max}$ ((µmol s^{-1} kg^{-1}) per body mass; corresponding to 0.744 $\dot{V}_{O_2,max}$ (ml min^{-1} kg^{-1})). Open and closed symbols, permeabilized fibers and isolated mitochondria. Regression lines are transformed from original graphs, representing the range of ergometric capacity in three studies. Full lines, Zoll et al. (2002) and Mettauer et al. (2001) (Table 2 – A; circles and diamonds: averages for sedentary, active or athletic fitness levels; $\dot{V}_{O_2,peak}$ is multiplied by 1.08; Tonkonogi and Sahlin, 1997). Dotted line, Tonkonogi and Sahlin (1997) (Table 2 – B; full square: average for athletic to sedentary). Full triangles, Mogensen et al. (2006) (Table 2 – A; untrained and trained; $\dot{V}_{O_2,peak}$ is multiplied by 1.08). Open triangle, Rabøl et al. (2009) (Table 2; obese, sedentary). Open square, Phielix et al. (2008) (Table 2 – B; overweight, sedentary).

mitochondrial activities in a comparable approach with isolated mitochondria (Tonkonogi and Sahlin, 1997) cannot be explained on the basis of aerobic fitness levels (Fig. 3, dotted line), and results reported by the same group with permeabilized fibres are similarly low (Table 2-B). Tissue-OXPHOS capacity obtained by Phielix et al. (2008) in sedentary overweight controls (Fig. 3, open square) is 32% of a morphometrically similar control group (Boushel et al., 2007), or 44% of obese controls studied under identical experimental conditions (Rabøl et al., 2009; Table 2). The aerobic capacity in these obese controls (Fig. 3, open triangle) fits well to the general dependence on maximal oxygen uptake in sedentary to athletic life styles. Sedentary controls with normal body mass index in the study of Hütter et al. (2007) have an apparent tissue-OXPHOS capacity that is only 50–60% of that in untrained subjects with normal body mass index (Bakkman et al., 2007), and the overweight aged group of Hütter et al. (2007) has only 40% of tissue-OXPHOS capacity of the comparable age group (75 and 72 years) of Rasmussen et al. (2003), or 50% of mitochondrial respiration per tissue mass in a sedentary overweight control group (Boushel et al., 2007). Hütter et al. (2007) observed a significant stimulation of respiration by cytochrome *c* in all subject groups in a protocol including octanoylcarnitine (Table 2), indicating an injury of the outer mitochondrial membrane in the permeabilized fibres at 37 °C, which was not the case when the same protocol was developed and applied at 30 °C (Gnaiger et al., 2005), or at 37 °C without addition of octanoylcarnitine (Boushel et al., 2007). $J_{O_2,P}$(GM) is less than 0.5 $J_{O_2,P}$(S) (Hütter et al., 2007), which might be due to partial depletion of NADH (Rustin et al., 1996) concomittant with cytochrome *c*, or due to inhibition of Complex I by residual rotenone contained in the oxygraph chamber. Loss of cytochrome *c* is one of the most common artefacts in isolation of mitochondria (Rasmussen and Rasmussen, 1997).

In patients used as controls (orthopedic hip replacement surgery, patients with lack of evidence for a manifest myopathy), $J_{O_2,P}$(CI+II, 37°C) is 45–70 pmol O_2 s^{-1} mg^{-1} wet weight, as measured with GMS (Kunz et al., 2000; 25 °C) or calculated from results with PM, GM and S(Rot) provided separately (Kunz et al., 1993; 25 °C; Sperl et al., 1997; 30 °C). These low mitochondrial capacities possibly reflect the low fitness level in these patients, or are partially influenced by methodological factors, such as oxygen limitation of respiration in permeabilized fibres (Gnaiger, 2003).

5. Conclusions: tissue-OXPHOS capacity and functional diversity

Substrate control is complementary to coupling control of oxygen flux in mitochondrial preparations, applied for assessment of physiological OXPHOS capacities and diagnosis of qualitative properties of mitochondrial respiratory control. The capacity of the electron transport system is generally underestimated on the basis of the 'State 3 paradigm' and conventional respiratory protocols applied with isolated mitochondria, permeabilized cells or tissues. The integrated function of the TCA cycle supports up to 2-fold higher fluxes through the electron transport system, with reconstituted convergent electron flow to the Q-junction through Complexes I + II, compared to respiration with either succinate + rotenone (electron input through Complex II) or NADH-related substrates alone (Fig. 2). Measurement with CI + II substrate supply at experimental temperature close to body temperature has to be considered as a standard for evaluation of $J_{O_2,P}$ in mammalian tissues.

Maximal oxygen uptake by quadriceps femoris is 220–260 µmol O_2 s^{-1} kg^{-1} in young adults with high ergometric fitness ($J_{O_2,max}$ from 40 to 47 µmol O_2 s^{-1} kg^{-1}; Andersen and Saltin, 1985; Rasmussen et al., 2001a; compare Fig. 3). Respiratory capacities measured in well coupled mitochondrial preparations, therefore, fall short of explaining the high respiratory capacity of human skeletal muscle *in vivo*, even when taking into account the temperature increase from 37 to 38 °C and corresponding stimulation of respiration by approximately 7%. This suggests a possible functional role of the apparent excess ETS over OXPHOS capacity in human skeletal muscle. In contrast to dissipative uncoupling, as applied in experimental evaluation of ETS capacity, maintenance of ion homeostasis in general, and Ca^{2+} cycling in particular, are functionally important energy demanding processes in excitable tissues. Rather than competing with oxidative phosphorylation of ADP to ATP, mitochondrial Ca^{2+} transport can additively stimulate respiration by utilizing the apparent excess ETS capacity. In vitro tissue-ETS capacity might povide the better estimate for the upper limit of mitochondrial respiration. Ca^{2+} at optimum concentration is an activator of dehydrogenases and oxidative phosphorylation, and a modest increase of free calcium concentration may stimulate respiration (Gueguen et al., 2005; Territo et al., 2000).

It is problematic to perform statistical evaluations of tissue-OXPHOS capacity in patients and controls without consideration of fitness level. Tissue-OXPHOS capacity at 37 °C with convergent electron input into the electron transport system is 60–120 pmol O_2 s^{-1} mg^{-1} in overweight adult humans with predominantly sedentary life style independent of age up to 70+ years. Tissue-OXPHOS capacity is pushed to the lower end of this range in obese subjects, but is increased to 100–180 pmol O_2 s^{-1} mg^{-1} in healthy subjects with normal body mass index, including top endurance athletes (Table 2). Mitochondrial biosynthesis adjusts OXPHOS capacity as an important component of the control of oxygen flux through the respiratory cascade from the lung, through the cardiovascular system to the mitochondria (di Prampero, 2003; Gnaiger et al., 1998; Weibel and Hoppeler, 2005). The strong increase of mitochondrial tissue capacity induced by exercise-training shifts the control of muscle oxygen uptake to oxygen supply to the tissue. In contrast, upon loss of mitochondrial capacity as the consequence of a sedentary lifestyle, mitochondrial OXPHOS capacity limits aer-

obic exercise capacity in untrained young individuals (Haseler et al., 2004) and contributes to the loss of aerobic power with advancing age in sedentary people (Short et al., 2005). Upregulation of proinflammatory cytokines such as TNF-α is associated with obesity as a state of chronic low-grade inflammation, disrupting the signalling cascade for mitochondrial biogenesis (Valerio et al., 2006). This molecular mechanism contributes, therefore, to the decline of tissue-OXPHOS capacity in the progression towards obesity (Fig. 3).

Considering the range from 60 to 180 pmol O_2 s^{-1} mg^{-1}, the tissue-OXPHOS capacity increases 3-fold from sedentary to athletic humans, comparable to the 2.7-fold difference of mitochondrial density between types I and IIb skeletal muscle (rabbit soleus and gracilis; Jackman and Willis, 1996). Mitochondrial volume per body mass and maximal oxygen consumption per body mass increase 2.5-fold when comparing athletic/sedentary animals (dog/goat; pony/calf; horse/steer; Weibel et al., 1991). This co-variation of functional capacity and mitochondrial density has established the paradigm that a higher respiratory capacity in skeletal muscle of mammalian species – from the 30 g mouse to the 500 kg horse – is achieved by simply building 'more mitochondria of the same kind' (Weibel et al., 1991; Weibel and Hoppeler, 2005). Comparison of $J_{O_2,P}$ versus $J_{O_2,E}$ (P/E coupling control ratios) and substrate control in mitochondria of human and mouse skeletal muscle, however, provides direct evidence for the fact that mitochondrial plasticity does not only involve a change in structure (mitochondrial density), but qualitative differences are highly significant in mitochondrial physiology of mouse (Aragonés et al., 2008) and man (Boushel et al., 2007). Further investigations of a wide range of species, tissues and fitness levels are required for describing the qualitative differences of mitochondria in terms of substrate control and coupling control. Without a proper comparative foundation of mitochondrial physiology, we cannot at present understand the functional implications of mitochondrial diversity from mouse to man, nor can we evaluate properly different tissue-OXPHOS and ETS capacities in health and disease.

Acknowledgements

I thank Robert Boushel, Hélène Lemieux, Steven Hand, Kathrin Renner, Dominique Votion, Bengt Kayser, Richard Haas, Charles Hoppel, Rodrigue Rossignol, Guy Brown and many unnamed colleagues for sharing their views on mitochondrial physiology during joint projects, numerous courses on high-resolution respirometry and Mitochondrial Physiology Conferences.

References

Andersen P, Saltin B. Maximal perfusion of skeletal muscle in man. J Physiol 1985;366:233–49.

Anderson EJ, Lustig ME, Boyle KE, Woodlief TL, Kane DA, Lin C-T, et al. Mitochondrial H_2O_2 emission and cellular redox state link excess fat intake to insulin resistance in both rodents and humans. J Clin Invest 2009;119:573–81.

Aragonés J, Schneider M, Van Geyte K, Fraisl P, Dresselaers T, Mazzone M, et al. Deficiency or inhibition of oxygen sensor Phd1 induces hypoxia tolerance by reprogramming basal metabolism. Nat Genetics 2008;40:170–80.

Bakkman L, Sahlin K, Holmberg HC, Tonkonogi M. Quantitative and qualitative adaptation of human skeletal muscle mitochondria to hypoxic compared with normoxic training at the same relative work rate. Acta Physiol (Oxford) 2007;190:243–51.

Bangsbo J, Gibala MJ, Howarth KR, Krustrup P. Tricarboxylic acid cycle intermediates accumulate at the onset of intense exercise in man but are not essential for the increase in muscle oxygen uptake. Pflugers Arch 2006;452:737–43.

Benard G, Bellance N, James D, Parrone P, Fernandez H, Letellier T, et al. Mitochondrial bioenergetics and structural network organization. J Cell Sci 2007;120:838–48.

Benard G, Faustin B, Galinier A, Rocher C, Bellance N, Smolkova K, et al. Functional dynamic compartmentalization of respiratory chain intermediate substrates: implications for the control of energy production and mitochondrdial diseases. Intl J Biochem Cell Biol 2008;40:1543–54.

Blomstrand E, Raedegran G, Saltin B. Maximum rate of oxygen uptake by human skeletal muscle in relation to maximal activities of enzymes in the Krebs cycle. J Physiol 1997;501:455–60.

Boushel R, Gnaiger E, Schjerling P, Skovbro M, Kraunsoe R, Flemming D. Patients with Type 2 diabetes have normal mitochondrial function in skeletal muscle. Diabetologia 2007;50:790–6.

Chance B, Williams GR. Respiratory enzymes in oxidative phosphorylation. IV. The respiratory chain. J Biol Chem 1955;217:429–38.

Chance B, Williams GR. The respiratory chain and oxidative phosphorylation. Adv Enzymol 1956;17:65–134.

Daussin FN, Zoll J, Dufour SP, Ponsot E, Lonsdorfer-Wolf E, Doutreleau S, et al. Effect of interval versus continuous training on cardiorespiratory and mitochondrial functions: relationship to aerobic performance improvements in sedentary subjects. Am J Physiol Regul Integr Comp Physiol 2008a;295:R264–72.

Daussin FN, Zoll J, Ponsot E, Dufour SP, Doutreleau S, Lonsdorfer E, et al. Training at high exercise intensity promotes qualitative adaptations of mitochondrial function in human skeletal muscle. J Appl Physiol 2008b;104:1436–41.

Dawson KD, Baker DJ, Greenhaff PL, Gibala MJ. An accute decrease in TCA cycle intermediates does not affect aerobic energy delivery in contracting rat skeletal muscle. J Physiol 2005;565:637–43.

di Prampero PE. Factors limiting maximal performance in humans. Eur J Appl Physiol 2003;90:420–9.

Echaniz-Laguna A, Zoll J, Ribera F, Tranchant C, Warter JM, Lonsdorfer J, et al. Mitochondrial respiratory chain function in skeletal muscle of ALS patients. Ann Neurol 2002;52:623–7.

Garnier A, Fortin D, Zoll J, N'guessan B, Mettauer B, Lampert E, et al. Coordinated changes in mitochondrial function and biogenesis in healthy and diseased human skeletal muscle. FASEB J 2005;19:43–52.

Gnaiger E. Bioenergetics at low oxygen: dependence of respiration and phosphorylation on oxygen and adenosine diphosphate supply. Respir Physiol 2001;128:277–97.

Gnaiger E. Oxygen conformance of cellular respiration. A perspective of mitochondrial physiology. Adv Exp Med Biol 2003;543:39–55.

Gnaiger E. (Ed.), Mitochondrial pathways and respiratory control. 1st ed. Innsbruck: OROBOROS MiPNet Publications; 2007. Electronic ISBN 978-3-9502399-0-4. www.oroboros.at.

Gnaiger E. Polarographic oxygen sensors the oxygraph and high-resolution respirometry to assess mitochondrial function. In: Dykens JA, Will Y, editors. Mitochondrial dysfunction in drug-induced toxicity. John Wiley; 2008. p. 327–52.

Gnaiger E, Kuznetsov AV, Schneeberger S, Seiler R, Brandacher G, Steurer W, et al. Mitochondria in the cold. In: Heldmaier G, Klingenspor M, editors. Life in the cold. Berlin, New York: Heidelberg Springer; 2000a. p. 431–42.

Gnaiger E, Lassnig B, Kuznetsov AV, Rieger G, Margreiter R. Mitochondrial oxygen affinity, respiratory flux control, and excess capacity of cytochrome *c* oxidase. J Exp Biol 1998;201:1129–39.

Gnaiger E, Méndez G, Hand SC. High phosphorylation efficiency and depression of uncoupled respiration in mitochondria under hypoxia. Proc Natl Acad Sci USA 2000b;97:11080–5.

Gnaiger E, Steinlechner-Maran R, Méndez G, Eberl T, Margreiter R. Control of mitochondrial and cellular respiration by oxygen. J Bioenerg Biomembr 1995;27:583–96.

Gnaiger E, Wright-Paradis C, Sondergaard H, Lundby C, Calbet JA, Saltin B, et al. High-resolution respirometry in small biopsies of human muscle: correlations with body mass index and age. Mitochondr Physiol Network 2005;10(9):14–5, www.mitophysiology.org/index.php?gnaigere.

Gueguen N, Lefaucheur L, Ecolan P, Fillaut M, Herpin P. Ca^{2+}-activated myosin-ATPases, creatine and adenylate kinases regulate mitochondrial function according to myofibre type in rabbit. J Physiol 2005;564:723–35.

Haseler LJ, Lin AP, Richardson RS. Skeletal muscle oxidative metabolism in sedentary humans: 31P-MRS assessment of O_2 supply and demand limitations. J Appl Physiol 2004;97:1077–81.

Hoppeler H, Howald H, Conley K, Lindstedt SL, Claassen H, Vock P, et al. Endurance training in humans: aerobic capacity and structure of skeletal muscle. J Appl Physiol 1985;59:320–7.

Hütter E, Skovbro M, Lener B, Prats C, Rabol R, Dela F, et al. Oxidative stress and mitochondrial impairment can be separated from lipofuscin accumulation in aged human skeletal muscle. Aging Cell 2007;6:245–56.

Jackman MR, Willis WT. Characteristics of mitochondria isolated from type I and type IIb skeletal muscle. Am J Physiol 1996;270:C673–678.

Johnson G, Roussel D, Dumas JF, Douay O, Malthièry Y, Simard G, et al. Influence of intensity of food restriction on skeletal muscle mitochondrial energy metabolism in rats. Am J Physiol Endocrinol Metab 2006;291:E460–7.

Jüllig M, Hickey AJ, Chai CC, Skea GL, Middleditch MJ, Costa S, et al. Is the failing heart out of fuel or a worn engine running rich? A study of mitochondria in old spontaneously hypertensive rats. Proteomics 2008;8:2556–72.

Kunz WS, Kudin A, Vielhaber S, Elger CE, Attardi G, Villani G. Flux control of cytochrome *c* oxidase in human skeletal muscle. J Biol Chem 2000;275:27741–5.

Kunz WS, Kuznetsov AV, Schulze W, Eichhorn K, Schild L, Striggow F, et al. Functional characterization of mitochondrial oxidative phosphorylation in saponin-skinned human muscle fibers. Biochim Biophys Acta 1993;1144:46–53.

Kuznetsov AV, Schneeberger S, Seiler R, Brandacher G, Mark W, Steurer W, et al. Mitochondrial defects and heterogeneous cytochrome *c* release after cardiac cold ischemia and reperfusion. Am J Physiol Heart Circ Physiol 2004;286:H1633–41.

Kuznetsov AV, Strobl D, Ruttmann E, Königsrainer A, Margreiter R, Gnaiger E. Evaluation of mitochondrial respiratory function in small biopsies of liver. Anal Biochem 2002;305:186–94.

Lemasters JJ. The ATP-to-oxygen stoichiometries of oxidative phosphorylation by rat liver mitochondria. J Biol Chem 1984;259:13123–30.

Lemieux H, Garedew A, Blier PU, Tardif J-C, Gnaiger E. Temperature effects on the control and capacity of mitochondrial respiration in permeabilized fibers of the mouse heart. Biochim Biophys Acta 2006;14:201–2, EBEC Short Reports Supplement.

Letellier T, Malgat M, Coquet M, Moretto B, Parrot-Roulaud F, Mazat JP. Mitochondrial myopathy studies on permeabilized muscle fibers. Pediatr Res 1992;32:17–22.

Mettauer B, Zoll J, Sanchez H, Lampert E, Ribera F, Veksler V, et al. Oxidative capacity of skeletal muscle in heart failure patients versus sedentary or active control subjects. J Am Coll Cardiol 2001;38:947–54.

Mitchell JH, Saltin B. The oxygen transport system and maximal oxygen uptake. In: Exercise physiology. Oxford Univ. Press; 2003.

Mitchell P, Moyle J. Respiration-driven proton translocation in rat liver mitochondria. Biochem J 1967;105:1147–62.

Mogensen M, Bagger M, Pedersen PK, Fernström M, Sahlin K. Cycling efficiency in humans is related to low UCP3 content and to type I fibres but not to mitochondrial efficiency. J Physiol 2006;571:669–81.

N'Guessan B, Zoll J, Ribera F, Ponsot E, Lampert E, Ventura-Clapier R, et al. Evaluation of quantitative and qualitative aspects of mitochondrial function in human skeletal and cardiac muscles. Mol Cell Biochem 2004;256–257:267–80.

Phielix E, Schrauwen-Hinderling VB, Mensink M, Lenaers E, Meex R, Hoeks J, et al. Lower intrinsic ADP-stimulated mitochondrial respiration underlies in vivo mitochondrial dysfunction in muscle of male type 2 diabetic patients. Diabetes 2008;57:2943–9.

Ponsot E, Zoll J, N'guessan B, Ribera F, Lampert F, Richard E, et al. Mitochondrial tissue specificity of substrates utilization in rat cardiac and skeletal muscles. J Cell Physiol 2005;203:479–86.

Puchowicz MA, Varnes ME, Cohen BH, Friedman NR, Kerr DS, Hoppel CL. Oxidative phosphorylation analysis: assessing the integrated functional activity of human skeletal muscle mitochondria – case studies. Mitochondrion 2004;4:377–85.

Rabøl R, Højberg PMV, Almdal T, Boushel R, Haugaard SB, Madsbad S, Dela F. Effect of hyperglycemia on mitochondrial respiration in type 2 diabetes. J Clin Endocrinol Metab 2009;94:1372–8.

Rasmussen HN, Rasmussen UF. Small scale preparation of skeletal muscle mitochondria, criteria for integrity, and assays with reference to tissue function. Mol Cell Biochem 1997;174:55–60.

Rasmussen UF, Rasmussen HN. Human quadriceps muscle mitochondria: a functional characterization. Mol Cell Biochem 2000;208:37–44.

Rasmussen UF, Rasmussen HN, Andersen AJ, Fogd Jorgensen P, Quistorff B. Characterization of mitochondria from pig muscle: higher activity of exo-NADH oxidase in animals suffering from malignant hyperthermia. Biochem J 1996;315:659–63.

Rasmussen UF, Krustrup P, Bangbo J, Rasmussen HN. The effect of high-intensity exhaustive exercise studied in isolated mitochondria from human skeletal muscle. Eur J Physiol 2001a;443:180–7.

Rasmussen UF, Krustrup P, Kjaer M, Rasmussen HN. Experimental evidence aginast the mitochondrial theory of aging: a study of isolated human skeletal muscle mitochondria. Exp Gerontol 2003;38:877–86.

Rasmussen UF, Rasmussen HN, Krustrup P, Quistorff B, Saltin B, Bangsbo J. Aerobic metabolism of human quadriceps muscle: in vivo data parallel measurements on isolated mitochondria. Am J Physiol Endocrinol Metab 2001b;280:E301–7.

Rasmussen UF, Vielwerth SE, Rasmussen HN. Skeletal muscle bioenergetics: a comparative study of mitochondria isolated from pigeon pectoralis, rat soleus, rat biceps brachii, pig biceps femoris and human quadriceps. Comp Biochem Physiol A Mol Integr Physiol 2004;137:435–46.

Richardson RS, Leigh JS, Wagner PD, Noyszewski EA. Cellular PO_2 as a determinant of maximal mitochondrial O_2 consumption in trained human skeletal muscle. J Appl Physiol 1999;87:325–31.

Rossignol R, Faustin B, Rocher C, Malgat M, Mazat JP, Letellier T. Mitochondrial threshold effects. Biochem J 2003;370:751–62.

Rostovtseva TK, Sheldon KL, Hassanzadeh E, Monge C, Saks V, Bezrukov SM, et al. Tubulin binding blocks mitochondrial voltage-dependent anion channel and regulates respiration. Proc Natl Acad Sci USA 2008;105:18746–51.

Rustin P, Parfait B, Chretien D, Bourgeron T, Djouadi F, Bastin J, et al. Fluxes of nicotinamide adenine dinucleotides through mitochondrial membranes in human cultured cells. J Biol Chem 1996;271:14785–90.

Saks VA, Veksler VI, Kuznetsov AV, Kay L, Sikk P, Tiivel T, et al. Permeabilised cell and skinned fiber techniques in studies of mitochondrial function in vivo. Mol Cell Biochem 1998;184:81–100.

Scandurra FM, Gnaiger E. Cell respiration under hypoxia: facts and artefacts in mitochondrial oxygen kinetics. Adv Exp Med Biol 2009.

Scheibye-Knudsen M, Quistorff B. Regulation of mitochondrial respiration by inorganic phosphate; comparing permeabilized muscle fibers and isolated mitochondria prepared from type-1 and type-2 rat skeletal muscle. Eur J Appl Physiol 2009;105:279–87.

Schwerzmann K, Hoppeler H, Kayar SR, Weibel ER. Oxidative capacity of muscle and mitochondria: Correlation of physiological, biochemical and morphometric characteristics. Proc Natl Acad Sci USA 1989;86:1583–7.

Short KR, Bigelow ML, Kahl J, Singh R, Coenen-Schimke J, Raghavakaimal S, et al. Decline in skeletal muscle mitochondrial function with aging in humans. Proc Natl Acad Sci USA 2005;102:5618–23.

Sperl W, Skladal D, Gnaiger E, Wyss M, Mayr U, Hager J, et al. High resolution respirometry of premeabilized skeletal muscle fibers in the diagnosis of neuromuscular disorders. Mol Cell Biochem 1997;174:71–8.

Starritt EC, Angus D, Hargreaves M. Effect of short-term training on mitochondrial ATP production rate in human skeletal muscle. J Appl Physiol 1999;86:450–4.

Territo PR, Mootha VK, French SA, Balaban RS. Ca^{2+} activation of heart mitochondrial oxidative phosphorylation: role of the F_0/F_1-ATPase. Am J Phyiol Cell Physiol 2000;278:C423–35.

Tonkonogi M, Harris B, Sahlin K. Mitochondrial oxidative function in human saponin-skinned muscle fibres: effects of prolonged exercise. J Physiol 1998;510:279–86.

Tonkonogi M, Sahlin K. Rate of oxidative phosphorylation in isolated mitochondria from human skeletal muscle: effect of training status. Acta Physiol Scand 1997;161:345–53.

Tonkonogi M, Walsh B, Tiivel T, Saks V, Sahlin K. Mitochondrial function in human skeletal muscle is not impaired by high intensity exercise. Eur J Physiol 1999;437:562–8.

Tudella VG, Curti C, Soriani FM, Santos AC, Uyemura SA. In situ evidence of an alternative oxidase and an uncoupling protein in the respiratory chain of *Aspergillus fumigatus*. Intl J Biochem Cell Biol 2003;36:162–72.

Turner DL, Hoppeler H, Claassen H, Vock P, Kayser B, Schena F, et al. Effects of endurance training on oxidative capacity and structural composition of human arm and leg muscles. Acta Physiol Scand 1997;161:459–64.

Valerio A, Cardile A, Cozzi V, Bracale R, Tedesco L, Pisconti A, et al. TNF-α downregulates eNOS expression and mitochondrial biogenesis in fat and muscle of obese rodents. J Clin Invest 2006;116:2791–8.

Veksler VI, Kuznetsov AV, Sharov VG, Kapelko VI, Saks VA. Mitochondrial respiratory parameters in cardiac tissue: a novel method of assessment by using saponin-skinned fibers. Biochim Biophys Acta 1987;892:191–6.

Walsh B, Tonkonogi M, Sahlin K. Effect of endurance training on oxidative and antoxidiative function in human permeabilized muscle fibres. Pflügers Arch 2001;442:420–5.

Weibel ER, Hoppeler H. Exercise-induced maximal metabolic rates scales with muscle aerobic capacity. J Exp Biol 2005;208:1635–44.

Weibel ER, Taylor CR, Hoppeler H. The concept of symmorphosis: a testable hypothesis of structure-function relationship. Proc Natl Acad Sci USA 1991;88:10357–61.

Wibom R, Hultman E, Johansson M, Matherei K, Constantin-Teodosiu D, Schantz PG. Adaptation of mitochondrial ATP production in human skeletal muscle to endurance training and detraining. J Appl Physiol 1992;73:2004–10.

Wijers SL, Schrauwen P, Saris WH, van Marken Lichtenbelt WD. Human skeletal muscle mitochondrial uncoupling is associated with cold induced adaptive thermogenesis. PLoS ONE 2008;3(3):e1777.

Zoll J, Sanchez H, N'Guessan B, Ribera F, Lampert E, Bigard X, et al. Physical activity changes the regulation of mitochondrial respiration in human skeletal muscle. J Physiol 2002;543:191–200.

MitoFit in health and protective medicine

Physical inactivity is one of the greatest drivers of metabolic dysregulation and preventable diseases in modern societies and has an impact on ageing populations in particular. It is becoming increasingly apparent that high and robust mitochondrial capacity is central to sustain metabolic health throughout life. An active lifestyle increases mitochondrial capacity and, therefore, reduces the risk of degenerative diseases.

High and efficient mitochondrial performance prevents metabolic diseases, promotes health and improves quality of life in ageing populations. Surprisingly, however, **there is currently no regimented, quantitative system or database dedicated to routinely test, compare and monitor mitochondrial function in individuals and populations.**

MitoFit

Tirol
Standortagentur

The project MitoFit is funded by the Land Tirol within the program K-Regio of Standort-agentur Tirol.

MitoFit develops novel laboratory standards and diagnostic monitoring of a mitochondrial fitness score. MitoFit provides a signature for high-end health tourism, introducing a scientific perspective on the benefits of mitochondrial fitness.

The OROBOROS O2k is the only instrument with sufficient stability and reliability for quantitative high-resolution respirometry (HRR). This world-leading technology introduced the quality control tools required for calibrated and standardised *in vitro* diagnostics – with the final aim to maintain mitochondria fit and well - to live a healthier, longer life.

MitoFit - diagnostic standard

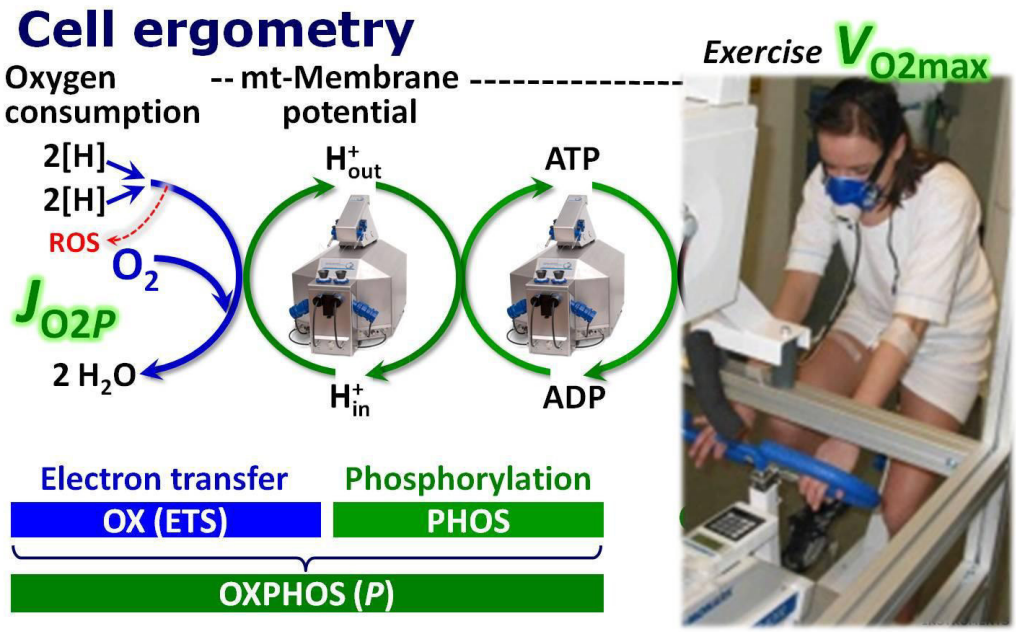

From spiroergometry (V_{O2max}) to cell ergometry for MitoFit scoring.

The O2k-Core and O2k-Fluorometer represent the gold standard for generating reliable quantitative respirometric data to develop the MitoFit Knowledge Management Platform (KMP) and MitoFit database.

- **Reference sample of cryopreserved mitochondria:** The availability of a reference sample for respirometry will provide enormous benefits for scientific research and open up new perspectives on clinical applications. Its use enables a new level of quality control in respiratory studies to be attained.
- **MitoFit proficiency test:** A ring test allows evaluation of the proficiency of a laboratory by measuring respiration of reference samples at pre-defined times and following standard experimental protocols. Reporting the reproducibility of measurements is a quality control for the evaluation of compliance with defined standard requirements.
- **MitoFit test on human blood cells:** Tissue biopsy for the study of mitochondrial function is a practical but invasive approach. Measurement of mitochondrial performance in human blood cells allows a noninvasive sampling procedure, enabling collection and cryopreservation of samples for later measurement and analysis. This will widen the applicability of respirometry for the study of human physiology immensly, permitting routine screening and repeated monitoring of the MitoFit score.

OROBOROS INSTRUMENTS
high-resolution respirometry
Schöpfstr 18, A-6020 Innsbruck, Austria
www.mitofit.org